УДК 533.9.01

STUDY OF HELIUM CRYOPLASMA

H.G. TARCHOUNA[1], N. BONIFACI[1], F. AITKEN[1], V.A. SHAKHATOV[2], V.M. ATRAZHEV[3], J. ELORANTA[4], F. JOMNI[5]

[1] *University Grenoble Alpes, Grenoble, France, E-mail: nelly.bonifaci@g2elab.grenoble-inp.fr*
[2] *Topchiev Institute of Petrochemical Synthesis RAS, E-mail: shakhatov@ips.ac.ru*
[3] *Joint Institute for High Temperatures RAS, Moscow,*
[4] *Department of Chemistry and Biochemistry, California State University, Northridge, USA,*
[5] *LabMOP, Campus Universitaire – El Manar, Tunis, Tunisia*

ИССЛЕДОВАНИЕ ГЕЛИЕВОЙ КРИОПЛАЗМЫ

Ч.Г. ТАРЧОНА[1], Н. БОНИФАСИ[1], Ф. ЭТКИН[1], В.А. ШАХАТОВ[2], В.М. АТРАЖЕВ[3], Ж. ЭЛОРАНТА[4], Ф. ИОМНИ[5]

[1] *Университет Гренобля, Гренобль, Франция,*
[2] *Институт нефтехимического синтеза им. А.В. Топчиева РАН, г. Москва,*
[3] *Объединенный институт высоких температур РАН, Москва,*
[4] *Калифорнийский университет, Нортридж, США*
[5] *ЛабМоп, Университет Эль-Манар, Тунис*

Summary

The properties of corona discharge were studied by electro-physical and spectral methods in the supercritical phase at 6 K, 11 K, 150 K and 300 K as well as in normal liquid helium at 4.2 K within the pressure range of 0.1-10 MPa. The light emitted from the ionization zone was analyzed. The rotational structure of the spectra was simulated to determine the rotational distribution function of excited He2-molecule.

Key words: corona discharge, liquid helium, ionization zone, rotational structure of the spectra.

Аннотация

Электрофизическими и спектральными методами были исследованы свойства коронного разряда в сверхкритической фазе при температуре 6 K, 11 K, 150 K и 300 K, а также в обычном жидком гелии при температуре 4.2 K при давлениях 0.1-10 МПа. Проанализировано излучение из зоны ионизации. Для определения вращательной функции распределения возбужденной молекулы He_2 была промоделирована вращательная структура спектра.

Ключевые слова: короннsый разряд, жидкий гелий, зона ионизации, молекулы водорода, вращательная структура спектра.

Introduction

Corona discharge is a simple method for injecting electrons in a dense cryogenic media such as the liquid helium. The discharge can be realized near a micron radius point electrode subject to a few kV potential. The light emission process in the discharge zone is believed to be initiated by electron avalanches in the strong field region leading to subsequent impact ionization of helium atom. The He^+ ions produced in the discharge interact rapidly with the surrounding atoms leading to the formation of He_2^+ dimer:

$$He^+ + He \rightarrow He_2^+$$

and the charge recombination event leads to the formation of diatomic excimer:

$$\mathrm{He}_2^+ + e^- \rightarrow \mathrm{He}_2^{**} .$$

Eventually, neutral excimers and, after further dissociation, excited He atoms are formed

$$\mathrm{He}_2^{**} \rightarrow \mathrm{He}^* + \mathrm{He} .$$

These excited He^* atoms and He_2^* excimers are the origin of the above mentioned luminescence

$$\mathrm{He}_2^{**} \rightarrow \mathrm{He}_2^* + h\nu ,$$

$$\mathrm{He}^{**} \rightarrow \mathrm{He}^* + h\nu .$$

The visible luminescence stems from the transitions between the electronically excited states of the above mentioned excited species whereas the VUV radiation involves termination directly to the electronic singlet ground state. Radiative transitions between electronically excited states in condensed matter systems have usually very low intensities due to the presence of fast electric dipole allowed relaxation channels. However, in helium such transition are either spin forbidden or have otherwise very low transition probability moments resulting in a rich emission spectrum within the atomic and diatomic excited states [1]. The spectroscopic observables are sensitive to the immediate surroundings of the emitting species, which makes emission spectroscopy a powerful tool for characterizing the cold nonequilibrium plasma as a function of pressure and temperature.

In this work, we have studied the current-voltage characteristics, spectral composition, and rotationally resolved molecular bands in corona discharge by using of the electro-physical and spectroscopic techniques.

1. Experimental set-up

The experimental set up consists of a helium cryostat, which allows measurements from the room temperature down to 4.2 K. A 50 Ohm coaxial beryllium copper cell equipped with a sapphire window was attached to the cryostat cold head, which allowed measurements up to 10 MPa.

The cell was first evacuated using a turbo molecular pump down to 10^{-4} Pa and then filled with ultra pure helium (N60 l'Air Liquide), which has an impurity concentration of less than 0.1 ppm of O_2. Prior entering the cell, helium gas was passed through a series of L-N_2 immersed traps, which were filled with a mixture of molecular sieves (3-10 Å) and activated charcoal (activation under vacuum for 3 days at 350° C).

The point electrode placed inside the cell was made of electrolytically-etched 1 mm diam. tungsten wire. Etching reduced the tip diameter to 0.45-2.5 micron, which was determined by electron microscope. The grounded plane electrode was made of copper and located 8 mm from the point electrode. All electrodes were carefully insulated with Macor ceramic.

The point electrode was either negatively or positively polarized by a stabilized high voltage DC power supply (Spellman RHSR/20PN60). The positive and negative corona discharges were driven by a positive or negative point electrode polarity, respectively. The current-voltage characteristics were measured by using a Tektronix TDS540 oscilloscope and a Keithley 610C Ampere meter.

The corona discharge in this geometry is axially symmetric and it appears as luminous spherical region (ionization region) localized near the point electrode against the dark background. The light originating from the ionization zone was collected by a quartz lens, focusing it onto the entrance slit of the spectrograph (Acton Research Corporation 300i equipped with gratings of 150 g/mm, 1200 g/mm blazed at 750 nm and of 1200 g/mm blazed at 300 nm). The measured intensity of the radiation was averaged over the observed line and the exposure time. A liquid N2 cooled 2D-CCDTKB-UV/AR detector was placed directly at the exit plane of the spectrograph. The noise level of the CCD detector is determined only by the read-out noise as the dark current of the camera is less than 1 e/pixel/h at 153 K.

The wavelength and intensity response of the detection system was calibrated by using a low pressure Helium (Lot Oriel SS.SPEC.He.10.0) and tungsten ribbon lamps. Line broadening due to the instrument response (1200 g/mm grating) was estimated from the helium lines of the lamp as $\Delta\lambda_{ins} = 0.12nm$.

2. Results and discussion

The negative corona current has been measured at different temperatures and pressures in the space-charge-limited regime. In this regime, the corona current I is quadratic with respect to the applied voltage V, i.e., plotting $I^{1/2}$ vs. V is linear with a slope proportional to the charge mobility μ (electrons for negative and positive ions for positive corona). This behavior was observed for negative corona in liquid helium ($= 4.2$ K) and supercritical helium (< 5.2 K).

The extracted electron mobilities are shown in Fig. 1. The determined charge mobility for the electron in normal liquid helium at 4.2 K is very low, 0.02 cm^2/Vs as compared with positive ions 0.053 cm^2/Vs [2]. This means that both electrons and positive ions have large effective masses in dense helium environments. On the contrary, in the gas phase electrons have much higher (kinetic) mobility as demonstrated in Fig. 1.

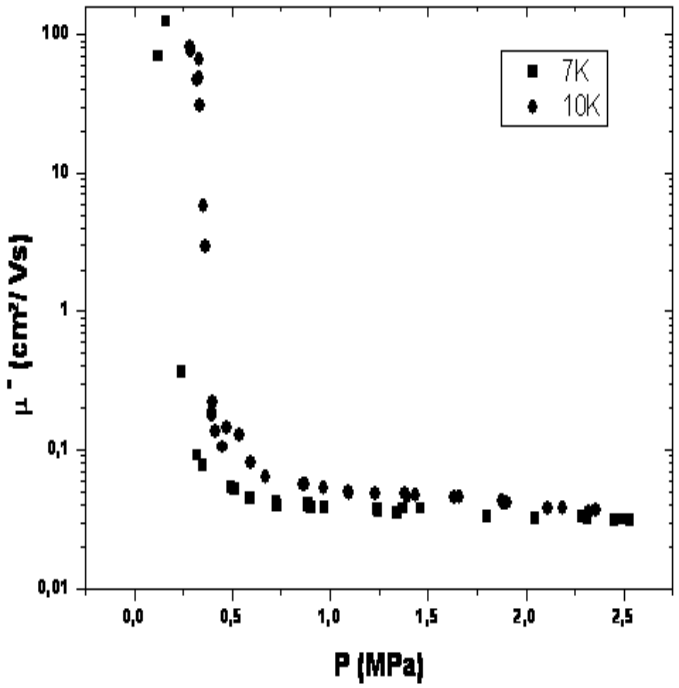

Fig. 1: Electron mobility in supercritical helium as a function of pressure

At the atomic level, this behavior can be rationalized through the repulsive interaction occurring between electrons and helium atoms and the formation of a positively charged helium clusters where additional ground state helium atoms may also bind by the charge – charge induced polarization interaction. In the gas phase, the electrons are quasi free and their mobility is determined by electron-helium scattering events whereas in the liquid phase, electrons localize in large bubbles (radius $\mathrm{R} \approx 20$ Å) [3] and the mobility is then determined by the Stokes'law. On the other hand, positive ions form charged helium clusters in both low temperature gas and liquid, and therefore the mobility is expected to depend much less on the surrounding helium density. The transition from the localized electron bubble state (low mobility) to the quasi free electron in gaseous helium is clearly observed between 0.1–0.5 MPa as shown in Fig. 1.

The measured radiation spectra of the corona discharge are shown in Figs. 2 and 3 at different temperatures. Spectral composition of the corona discharge strongly depends on temperature. Intensities have not been corrected for the spectral response of the detection system. Most of the observed bands could be assigned through a comparison with the room – temperature gas phase spectra of Ginter [4, 5].

Spectral line of atomic helium He ($3s^3\mathrm{S}$-$2p^3\mathrm{P}$), bands of molecular helium He_2 ($e^3\Pi_g$-$a^3\Sigma_u^+$ and $J^1\Delta_u$-$B^1\Pi_g$) are observed in the wavelength range 456-480 nm (Fig. 2). Figure 4 illustrates the energy level diagram.

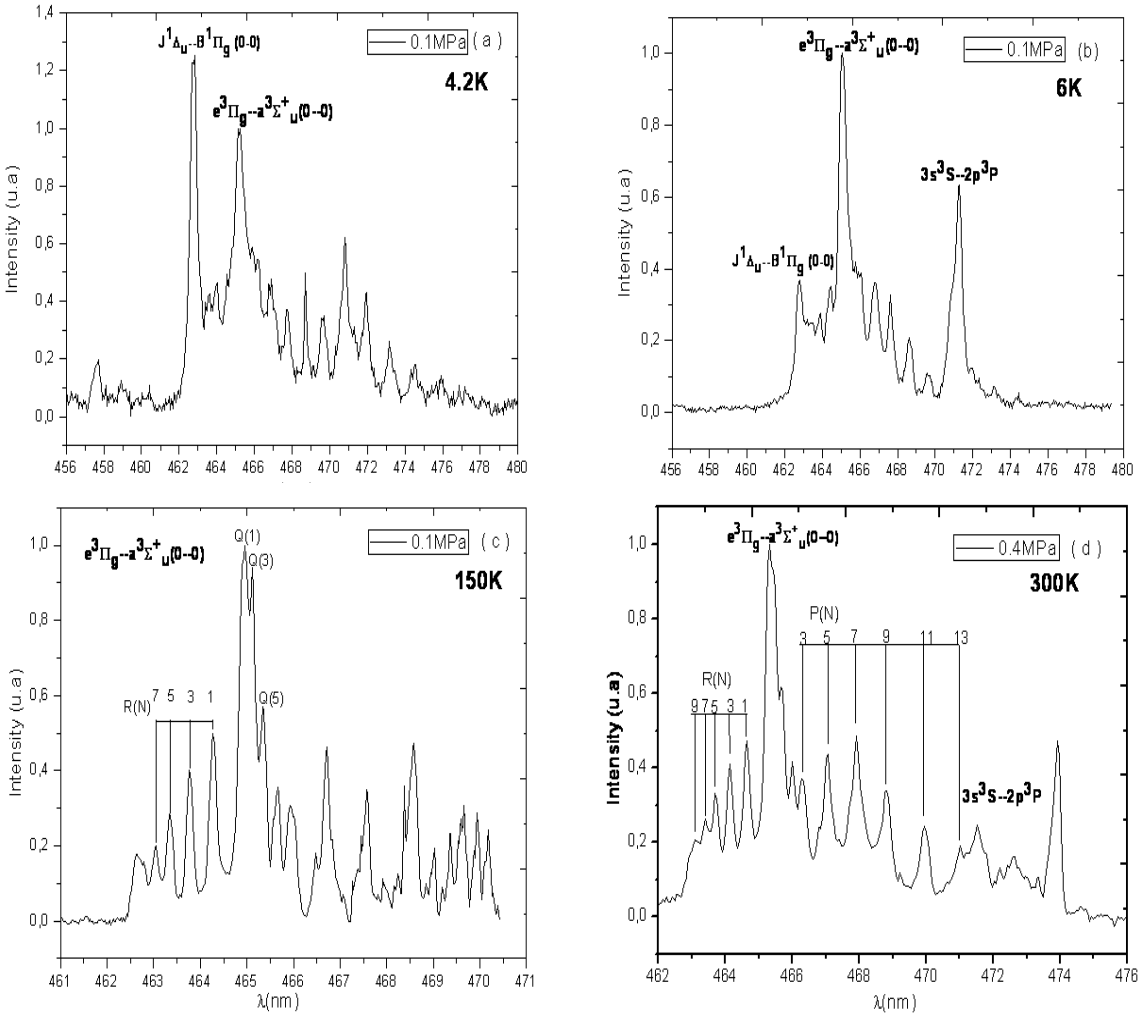

Fig. 2: Bands of the triplet $e^3\Pi_g - a^3\Sigma_u^+$ and singlet $J^1\Delta_u - B^1\Pi_g$ transitions.

Important effect of temperature at 0.1 MPa can be seen of the triplet $e^3\Pi_g - a^3\Sigma_u^+$ molecular band transitions. For the lower temperature 4.2 and 6 K this band present singlet band, but with increasing temperature the triplet transition are clear, different R or Q – branches are observed. Also band of the He_2 ($J^1\Delta_u - B^1\Pi_g$) appears at 4.2 at 6 K disappears at 150 and 300 K. This effect can be caused by the type of molecular interaction. Intense rotationally resolved bands of He_2 ($C^1\Sigma_g^+$ - $A^1\Sigma_u^+$ and $c^3\Sigma_g^+ - a^3\Sigma_u^+$) that belong to $\Delta v = 0$ vibrational transitions can be clearly identified between 900 and 970 nm (Fig. 3). The panels (a) and (b) of Fig. 3 show a magnification of the selected regions belonging to the general overview spectrum of panel (c). The singlet and triplet state He_2^* potentials corresponding to the C-A and c-a transitions are very similar to each other and therefore the bands overlap complicating the spectral analysis [5, 6]. The intensity of the triplet transition $c^3\Sigma_g^+$ ac $^3\Sigma_u^+$ is well higher than that of the corresponding singlet transition $C^1\Sigma_g^+$ $A^1\Sigma_u^+$. Fig. 3 (a)-(c) shows the line intensities and positions belonging to the rotational bands in both singlet and triplet manifolds as function of temperature. A considerable number of the rotational lines, which are attributed to the upper radiative triplet $c^3\Sigma_g^+$ and singlet $C^1\Sigma_g^+$ excited states, are observed in the spectra at 6 K and 11 K. Note that the similar saturation of the spectra in the investigated range by the rotational lines of the strong intensities was also found in study of helium nanodroplets and recombination in low temperature helium gas [7, 8]. The models usually presented to explain the origin of the highly rotationally excited states in the gas all involve ion-electron recombination, e.g., of He_3^+ [9].

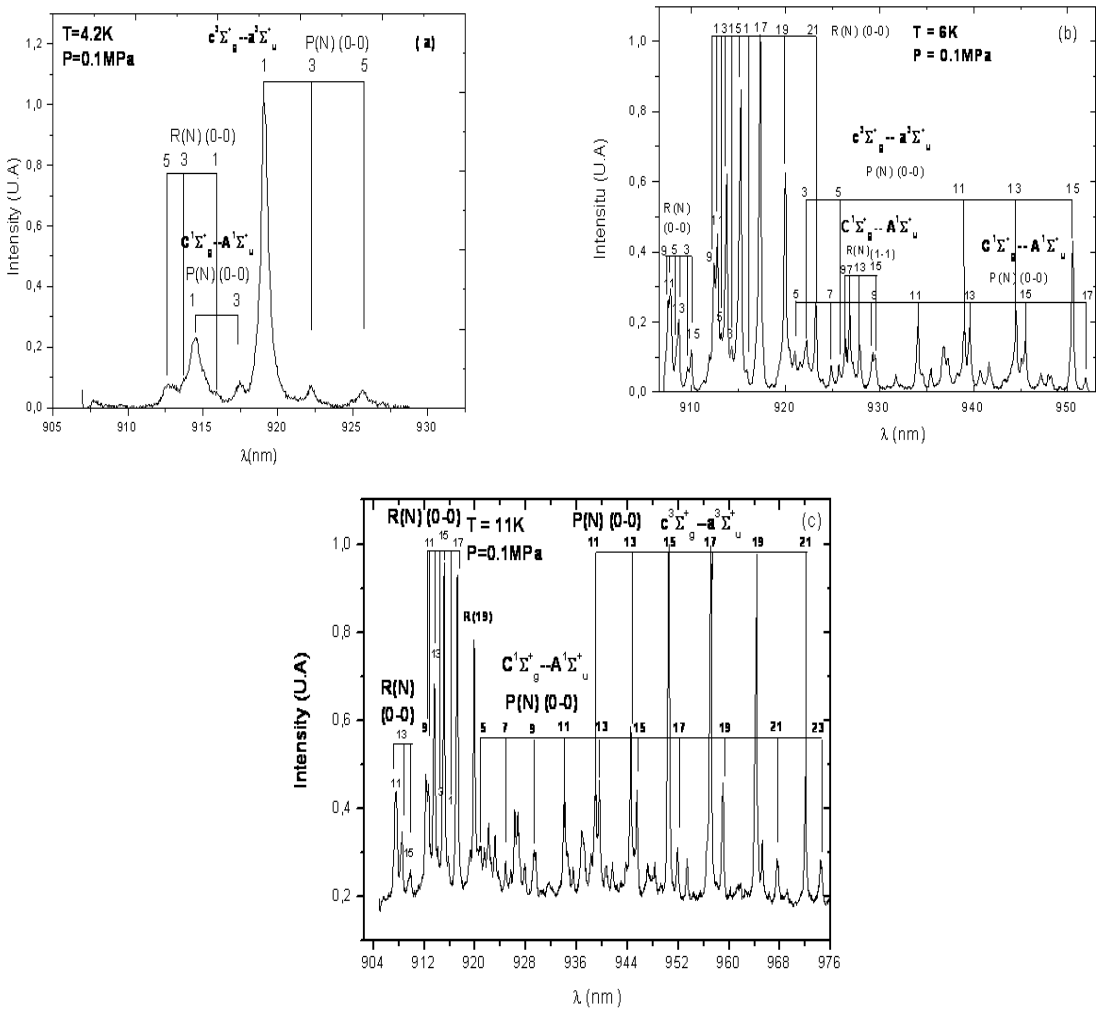

Fig. 3: Position of the rotational lines for (0-0) and (1-1) bands of the triplet $c\,^3\Sigma_{g^-}\,a\,^3\Sigma_u^+$ and singlet $C\,^1\Sigma_{g^-}$ $A\,^1\Sigma_u^+$ transitions.

This enables one to use the method of amplitudes (Boltzmann's plot technique) and reliably determine the rotational distribution function of helium molecules in the singlet and triplet excited states. The experimentally obtained spectrum is used to determine the dependence of $\ln\left[I_{k'k''}/(\nu^4_{k'k''}S_{k'k''})\right]$ on the values of $E_{k'}$ (here, $I_{k'k''}$ is line intensity, $\nu_{k'k''}$ is the frequency of the radiation, $S_{k'k''}$ is the appropriate Hönl-London factor, $E_{k'}$ is the energy for the upper vibrational level, k' and k'' are the rotational quantum numbers of the upper and low levels, respectively).

The recovered rotational distribution functions are given in Fig. 5. The functions are differed from the Boltzmann distributions.

3. Conclusion

In this work, we studied the properties of corona by using electro-physical and spectral methods in the supercritical phase at 6 K and 11 K as well as in normal liquid helium at 4.2 K within the pressure range of 0.1-10 MPa. It is established that: charge mobilities (for electrons and positive ions) decrease as a function of external pressure in both supercritical and liquid phases of helium; charge mobility for the electron in normal liquid helium at 4.2 K is very low, as compared with positive ions; the spectral composition of the

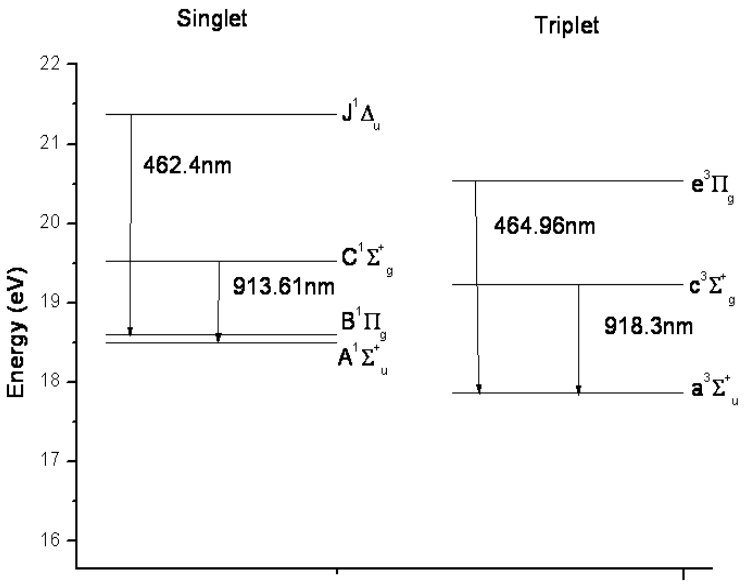

Fig. 4: The energy level diagram of molecular helium.

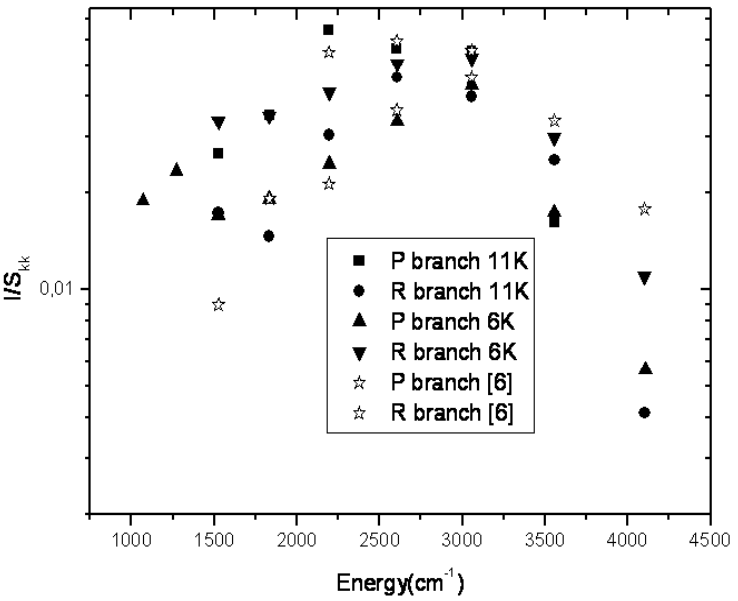

Fig. 5: Values of $\ln\left[I_{k'k''}/(\nu^4_{k'k''}S_{k'k''})\right]$ against $E_{k'}$ plot of the intensities in the P and R branches of the triplet $c^3\Sigma^+_{g-}\, a^3\Sigma^+_u$ transition.

corona discharge strongly depends on temperature; the rotational distribution functions, determined from the distributions of transition intensities of the He_2 ($c^3\Sigma^+_{g-}\, a^3\Sigma^+_u$) are differ from the Boltzmann distributions. Further experiments and calculations are required to better understand the origin of the appearance and disappearance of the variation of their intensity.

Acknowledgment

V.A.S. and V.M.A. thank the Russian Foundation of Basic Researches for support of their work, grant 12-08-91052. Financial support to J.E. from the National Science Foundation grants CHE-1262306 and DMR-1205734 are also acknowledged.

REFERENCES

1. **Li Z., Bonifaci N., Aitken F., Denat A., Von Haeften K., Atrazhev V.M., Shakhatov V.A.** // Eur. Phys. J. Appl. Phys. – 2009. – V. 47. – P. 22821.
2. **Li Z., Bonifaci N., Denat A., Atrazhev V.M.** // IEEE Trans. on Dielectrics and Electrical Insulation. – 2006. – V. 13. – P. 624.
3. **Fetter A.L.** In «The Physics of liquid and solid Helium» / Benneman K.H. and Ketterson J.B., Eds. – NY: Wiley, 1976.
4. **Brown C., Ginter M.** // Journal of Molecular Spectroscopy. – 1971. – V. 5. – P. 302.
5. **Ginter M.L.** // J. Chem. Phys. – 1965. – V. 42. – P. 561.
6. **Kafanov S.G., Parshin A.Ya., Todoshchenko I.A.** // JETP. – 2000. – V. 91. – P. 991.
7. **Yurgenson S., Hu C.C., Kim C., Northby J.A.** // Eur Phys. J.D. – 1999. – V. 9. – P. 153.
8. **Callear A.B., Hedges R.E.M.** // Nature. – 1967. – V. 215. – P. 1267.
9. **Tokaryk D.W., Brooks R.L., Hunt J.L.** // Phys. Rev. A. – 1993. – V. 48. – P. 364.